Journal of Physics G: Nuclear and Particle Physics

Measurement of fusion cross sections for $^{16}O+^{16}O$

IOP Publishing Journal of Physics G: Nuclear and Particle Physics

J. Phys. G: Nucl. Part. Phys. **42** (2015) 065102 (10pp) doi:10.1088/0954-3899/42/6/065102

Measurement of fusion cross sections for $^{16}O+^{16}O$

J G Duarte[1], L R Gasques[1], J R B Oliveira[1], V A B Zagatto[1], L C Chamon[1], N H Medina[1], N Added[1], W A Seale[1], J A Alcántara-Núñez[1], E S Rossi Jr[1,2], P Amador-Valenzuela[3], A Lépine-Szily[4], A S Freitas[1], V Scarduelli[1], V A P Aguiar[1] and J M B Shorto[5]

[1] Departamento de Física Nuclear, Instituto de Física da Universidade de São Paulo, Caixa Postal 66318, 05315-970, São Paulo, SP, Brazil
[2] Centro Universitário FIEO—UNIFIEO, Osasco, SP, Brazil
[3] Departamento de Aceleradores, Instituto Nacional de Investigaciones Nucleares, Apartado Postal 18-1027, Código Postal 11801, México, Distrito Federal, México
[4] Departamento de Física Experimental, Instituto de Física da Universidade de São Paulo, Caixa Postal 66318, 05315-970, São Paulo, SP, Brazil
[5] Instituto de Pesquisas Energéticas e Nucleares—IPEN, 05508-000 São Paulo, Brazil

E-mail: lgasques@if.usp.br

Received 3 February 2015, revised 9 March 2015
Accepted for publication 23 March 2015
Published 7 May 2015

Abstract

In earlier works, the fusion cross section for the $^{16}O+^{16}O$ reaction has been measured using different techniques. In the present work, we have obtained an experimental excitation function for $^{16}O+^{16}O$ using γ-ray spectroscopy. The measurements were performed at center-of-mass energies between 8.28 and 12.25 MeV. The theoretical predictions obtained with a coupled-channel model are consistent with the experimental data. From our analyses, the extrapolated S-factor value at 6.6 MeV, corresponding to the Gamow peak energy for core oxygen burning conditions, is about 3.6×10^{25} MeV barn.

Keywords: fusion, γ-spectroscopy, coupled-channel

(Some figures may appear in colour only in the online journal)

1. Introduction

Thermonuclear reactions in the interior of a main sequence star begin with the hydrogen burning phase, when four protons combine to form a helium nucleus. The nuclear energy produced by these reactions counteracts the gravitational force, maintaining the star in

equilibrium. As the fuel is exhausted, the core of the star starts to collapse, transforming gravitational potential energy into heat. Depending on the mass of the star, its core can accumulate sufficient energy to ignite the ashes of the previous phase, which will become fuel for the next burning stage. For sufficiently massive stars, the nuclear burning proceeds until the helium and heavier elements up to iron are formed. After helium has been exhausted in the core of the star, carbon, neon and oxygen burning phases take place, followed by the silicon burning phase. These are the major burning stages leading to the nucleosynthesis of elements with $A \geqslant 20$. In the carbon burning phase of a massive star ($M \gtrsim 8M_{\odot}$), the most important reaction is the ^{12}C+ ^{12}C fusion [1]. However, depending on the ^{12}C/^{16}O abundance ratio, which is determined by the ^{12}C(α, γ)^{16}O reaction rate, additional processes such as ^{12}C+^{16}O and ^{16}O+^{16}O may occur [2, 3]. At sufficient high temperatures ($\gtrsim 10^9$ K), the oxygen burning phase can proceed mainly through the ^{16}O+^{16}O reaction, leading to the formation of a variety of residual nuclei ranging from magnesium to sulfur, which will be consumed in the succeeding silicon burning phase.

Considerable discrepancies among different experimental data sets of the fusion cross sections for the ^{12}C+^{12}C, ^{12}C+^{16}O and ^{16}O+^{16}O reactions make the situation rather uncertain at sub-barrier energies. Typically, the reactions of astrophysical interest take place at energies far below the Coulomb barrier (around the Gamow energy) [4], where it is difficult to obtain experimental data with high accuracy due to the low cross sections associated. A few decades ago, the ^{16}O+^{16}O reaction was widely explored using different experimental techniques [5–10]. Although most of the experiments were planned to measure secondary γ-rays from the evaporation residues, some detected the evaporated light particles from the compound nucleus. The available data at energies around the Gamow peak, corresponding to temperatures typical for core oxygen burning ($T \sim 2.2$ GK; $E_0 \sim 6.6 \pm 1.3$ MeV) and explosive oxygen burning ($T \sim 3.6$ GK; $E_0 \sim 9.2 \pm 2.0$ MeV), are in poor agreement as the ratio between the highest and lowest value of cross section reaches a factor of about 3 in the lowest energy region [10–12]. As the fusion cross sections are input parameters in many stellar evolution codes, their insufficiently precise knowledge at energies relevant to astrophysics can result in huge uncertainties in the reaction rate between the ^{16}O nuclei. To disentangle these discrepancies, higher quality data are needed. In this work, we have measured the fusion cross section for ^{16}O+^{16}O in the energy range between 8.28 and 12.25 MeV in the center-of-mass frame of reference using the γ-spectroscopy technique.

It is well known that, at energies not too far below the Coulomb barrier, sub-Coulomb fusion cross sections present an enhancement in comparison with predictions obtained using a simple one-dimensional barrier penetration model (BPM) [13, 14]. Couplings to the inelastic channels are usually taken into account in fusion cross section calculations to explain the effect of the internal structure of the colliding nuclei. This formalism has been successful in describing many heavy-ion systems [15–17]. In the present work, we have performed coupled-channel (CC) calculations, assuming the parameter-free São Paulo potential [18] as the bare interaction. The experimental data are in good agreement with the CC results.

2. Experimental method

The experiment was performed at the Laboratório Aberto de Física Nuclear of the University of São Paulo, where secondary γ-rays from the evaporation residues of the ^{16}O+^{16}O reaction were measured. As shown schematically in figure 1, the experimental arrangement was composed of two high-purity germanium (HPGe) detectors located at 55° and 125°, used to measure secondary γ-rays emitted by the evaporation residues. Both HPGe detectors were

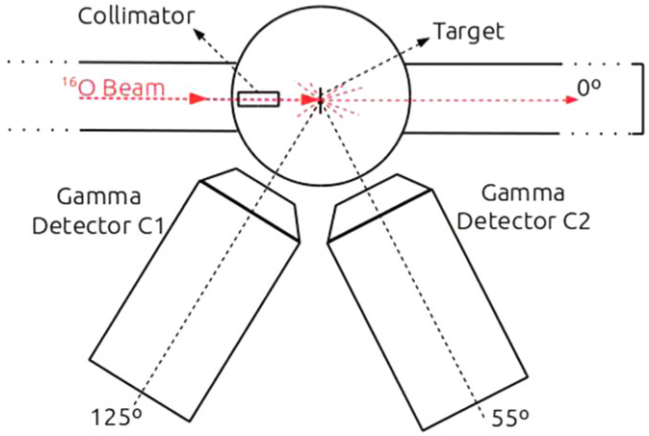

Figure 1. Schematic diagram of the arrangement used to measure the fusion cross section for the ^{16}O+^{16}O reaction.

coupled to a Compton-suppression system used to improve the signal to background ratio in the spectrum [19, 20]. In general, γ-emission presents an angular distribution which is not isotropic in the laboratory frame. In our experiment, the angles of the detectors were chosen to minimize the effects of possible anisotropies in the γ emission [6, 21]. Furthermore, the direct comparison of the spectra obtained with each detector allows the identification of Doppler shift events. The typical energy resolution of the HPGe detectors was about 2.3 keV. The relative photopeak efficiency of the HPGe detectors was determined by the use of a ^{152}Eu radioactive source placed at the target position. The HPGe detectors were mounted at 19 cm from the target, which corresponds to the closest possible geometry for the experimental setup. In an attempt to reduce the natural background, the detector placed at 55° was shielded with 5 cm of lead. Because of geometric limitations, we could not add more lead bricks to improve the shielding of the detector. It turned out that the comparison between the spectra obtained with and without shielding showed an almost negligible effect for the entire energy region of the experiment. Spectra with no beam hitting the target were taken during and after the experiment. These spectra were used to subtract the background of the in-beam spectra acquired at different incident energies. An inspection of the no beam spectra also indicated the absence of γ lines coming from contamination of the target.

The accelerated ^{16}O beams, with energies ranging from E_{Lab} = 17.0 to 25.0 MeV, were incident on an oxygen target made through the evaporation of molybdenum oxide on gold backing foil. To determine the thickness of the targets, we have measured their depth profile by the Rutherford backscattering method. Typically, the targets were produced with a thickness of 0.15 mg cm^{-2} of molybdenum oxide and 0.7 mg cm^{-2} of gold. To normalize the fusion cross section data, we have used the 279 and 536 keV γ-rays produced by the Coulomb excitation of ^{197}Au and ^{100}Mo, respectively. The results obtained in both cases are compatible within the statistical errors of the experiment.

3. Experimental results

A typical γ-ray spectrum, where all the important γ-ray lines are indicated, is shown in figure 2. Most of the peaks used to determine the partial cross sections are Doppler shifted. As

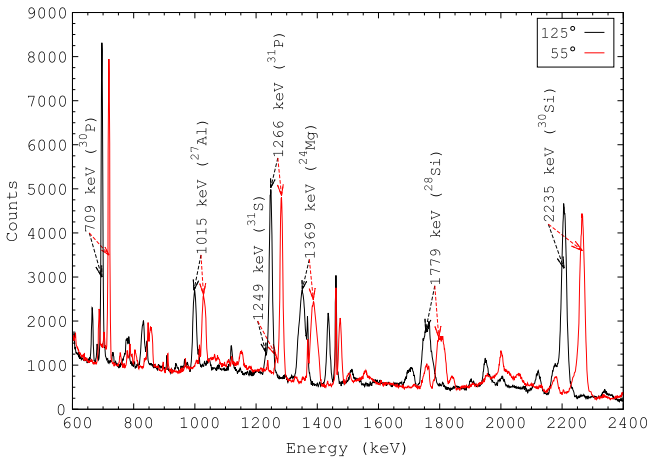

Figure 2. Typical γ-ray spectra obtained with the detectors placed at 55° and 125° at $E_{\mathrm{c.m.}}$= 25 MeV. The important γ-lines are identified in the figure. The peaks are Doppler shifted.

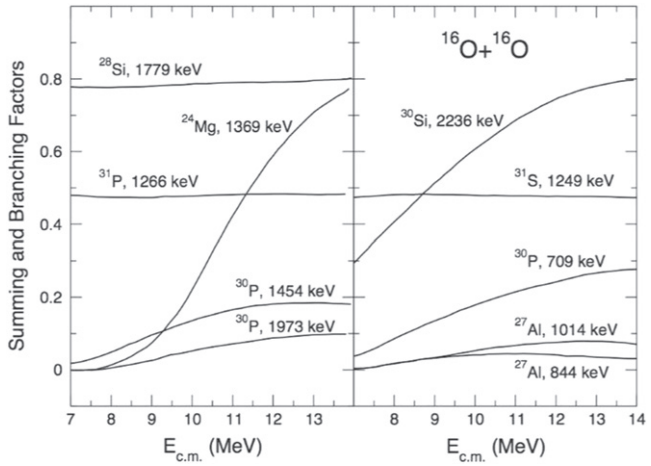

Figure 3. The summing and branching factors as a function of the center-of-mass energy for the γ-ray transitions of the residual nuclei produced by the ^{16}O+^{16}O reaction.

previously mentioned, the identification of the peaks was carried out by comparing the spectra obtained with both HPGe detectors, which were strategically located at 55° and 125°. For most of the residual nuclei formed in excited states, more than a single γ-ray were observed due to the deexcitation of different levels populated in the ^{16}O+^{16}O reaction. In our analysis, we have determined the partial cross sections using only the most intense γ-ray line for each exit reaction channel. The corresponding yields were corrected by considering the probability of populating higher lying levels in the residual nucleus. To this aim, we have used the summing and branching factors (BFs) reported in [9], which were calculated by considering the Hauser–Feshbach statistical model formalism [22]. The BF for the γ-ray transitions of the residual nuclei of interest are plotted as a function of the center-of-mass energy in figure 3. As can be observed from the figure, the BF for the nuclei evaporating two light particles present a

Table 1. Parameters obtained by fitting the relative efficiency data.

Parameter	Detector $C1$	Detector $C2$
A	−46.3972	0.515257
B	27.7603	2.067090
C	−2.99218	0.180125
D	−0.448556	−0.030578
E	0.105992	−0.009118
F	−0.005495	0.000962

Table 2. Gamma peaks used for the analysis.

Energy (keV)	Half-life (ps)	Nucleus
1249	0.5	^{31}S
1266	0.523	^{31}P
2235	0.215	^{30}Si
709	45	^{30}P
1779	0.475	^{28}Si
1015	1.49	^{27}Al
1369	1.33	^{24}Mg

strong variation with the energy. For the energy range in which the experiment was performed, all residual nuclei are formed with excitation energy above the ground state, even though some channels have negative Q-values. Therefore, transitions that only emit particles without γ-rays are very unlike. As shown in [7], the agreement of the fusion cross section data for the ^{16}O+^{16}O obtained through γ-ray spectroscopy and by detecting the evaporated light particles from the compound nucleus is satisfactory within the statistical errors of the experiments.

In general, the partial fusion cross section can be obtained from the relation:

$$\sigma_{\gamma}^{\mathrm{ch}} = \frac{Y_{\gamma}^{\mathrm{ch}}}{N_i N_t \, \beta_{\gamma}^{\mathrm{ch}} \, \epsilon_{\gamma}^{\mathrm{absolute}}}, \tag{1}$$

where Y_{γ}^{ch} is the yield for a particular channel, N_i is the number of incident nuclei, N_t is the number of oxygen atoms per unit of area of the target, $\beta_{\gamma}^{\mathrm{ch}}$ is the BF and $\epsilon_{\gamma}^{\mathrm{absolute}}$ the absolute efficiency. As aforementioned, in this work, we have measured the relative efficiency (ϵ_{γ}) of each HPGe detector using radioactive sources of ^{152}Eu and ^{133}Ba. This quantity, which depends on the γ-ray energy (E_{γ}), can be represented by the equation [23]:

$$\begin{aligned} \epsilon_{\gamma} &= \exp\left[A + Bx + Cx^2 + Dx^3 + Ex^4 + Fx^5\right]; \\ x &= \ln\left(E_{\gamma}\right). \end{aligned} \tag{2}$$

The parameters obtained by fitting the relative efficiency data are presented in table 1.

To obtain a relative normalization of the fusion cross section for each channel and energy, we have used the Coulomb excitation cross sections for ^{197}Au or ^{100}Mo:

$$\sigma_\gamma^{\mathrm{ch}} = \sigma_\gamma^{\mathrm{CE}} \frac{Y_\gamma^{\mathrm{ch}} \epsilon_\gamma^{\mathrm{CE}}}{Y_\gamma^{\mathrm{CE}} \epsilon_\gamma^{\mathrm{ch}} \beta_\gamma^{\mathrm{ch}}}, \tag{3}$$

where $\sigma_\gamma^{\mathrm{CE}}$ is the Coulomb excitation cross section calculated using the CCs code FRESCO [24] and Y_γ^{CE} is the yield corresponding to the Coulomb excitation of ^{197}Au or ^{100}Mo. The partial fusion cross sections obtained with the 279 keV γ-ray line of ^{197}Au and the 536 keV γ-ray line of ^{100}Mo agree within the statistical errors of the experiment. The characteristic γ-ray transitions used to obtain the partial cross sections are given in table 2.

To avoid carbon buildup on the target, it is necessary to ensure that ultra-high vacuum conditions are maintained in the vicinity of the target. In our experiment, the typical vacuum was around 10^{-7} Torr, which is probably insufficient to completely avoid carbon buildup. A comparison of two spectra measured at 25 MeV at the beginning and at the end of our experiment reveals a clear signature of carbon buildup on the target during the experiment. The consequences of the presence of carbon on the target will be discussed in the following.

The peak at 1779 keV is attributed to the deexcitation of ^{28}Si, where the major part of the peak is Doppler shifted. Lying in the same region of the spectra, there is a peak at 1808 keV that is also Doppler shifted. This peak comes from the contribution of ^{26}Mg formed in the reaction of ^{16}O with ^{12}C, which is a contamination in our target. In the spectra of the detector placed at 125°, we observed that the unshifted peak at 1779 keV overlaps with the Doppler peak at 1808 keV. Conversely, in the spectra of the detector placed at 55° we observed the Doppler peak of 1779 keV overlapped with the stop peak of 1808 keV. For this reason, we could not determine the partial cross section for the ^{28}Si residual nucleus. To resolve this problem, we have adopted the partial cross section for this particular channel from the literature [9].

The peaks at 1015 and 1369 keV were attributed to ^{27}Al and ^{24}Mg respectively. Their yields are 60(3)% at the Doppler peak and 40(3)% at the unshifted peak. These residual nuclei can come either from ^{16}O+^{16}O or from ^{16}O+^{12}C. In order to obtain the partial cross sections for ^{24}Mg and ^{27}Al, which are exclusively related to the ^{16}O+^{16}O reaction, we have to remove the contribution of these channels coming from the reaction with the carbon contamination. For this purpose, we have used the experimental cross sections for ^{24}Mg, ^{26}Mg and ^{27}Al reported in [25], to infer the yields of these channels which are related to the ^{16}O+^{12}C reaction.

The total fusion cross section was calculated by the relation:

$$\sigma_{\mathrm{total}}^{E_{\mathrm{eff}}} = \Gamma \sum \sigma_\gamma^{\mathrm{ch}}, \tag{4}$$

where Γ is an energy independent normalization factor, which was determined matching the experimental and the CC theoretical fusion cross sections at the highest energy. At low energies, typical for astrophysical conditions, fusion cross sections are often expressed in terms of the so-called astrophysical S-factor

$$S(E) = E\, \sigma(E) \exp(2\pi\eta), \tag{5}$$

$$\eta = \frac{e^2 Z_1 Z_2}{\hbar} \left(\frac{\mu}{2E} \right)^{\frac{1}{2}}, \tag{6}$$

where η is the Sommerfeld parameter, e is the elementary charge, Z_1 and Z_2 are the charge numbers of the nuclei, and μ is the reduced mass of the system.

To determine the effective bombarding energy of the beam, a correction due to the thickness of the target must be considered. In the present work, the bombarding energy (E_0) has been corrected by assuming an exponential decrease of the cross section value from σ_1 at

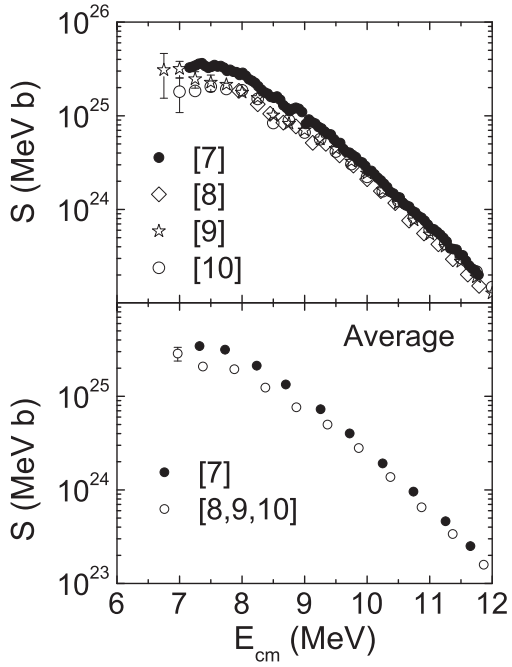

Figure 4. (top) Experimental data for the fusion cross section for the ^{16}O+^{16}O reaction represented in terms of the astrophysical *S*-factor. (bottom) Averaged astrophysical *S*-factor in bins of 500 keV.

E_0 to σ_2 at $E_0 - \Delta$, where Δ is the total energy loss in the target. Table 3 contains the experimental results for the fusion cross sections and the astrophysical *S*-factors obtained in the present work.

4. Discussion

Many experiments have been performed to measure the fusion cross section for the ^{16}O+^{16}O reaction. Discrepancies among the available cross section data reach up to a factor of 3, as represented in the upper panel of figure 4 in terms of the astrophysical *S*-factor. The data set of Spinka and Winkler [7] cover the energy region of $7.16 \leqslant E_{\mathrm{c.m.}} \leqslant 11.83$ MeV, measured with steps of 50 keV. The data of [7] are systematically above the experimental results obtained in other works [8–10]. To emphasize this point, an averaged astrophysical *S*-factor was calculated in bins of 500 keV for the data set of Spinka and Winkler [7] and for the data sets of [8–10]. The results are shown in the bottom panel of figure 4. As shown in figure 5, the data obtained in the present work are in accord with the averaged astrophysical *S*-factor corresponding to the data sets reported in [8–10]. In particular, our datum at the lowest energy is in quite good agreement with the average value of [8–10], but its error bar makes it marginally compatible also with the data set of Spinka and Winkler (see figure 5).

For heavy-ion reactions, fusion cross sections at energies below the Coulomb barrier present large enhancements in comparison with the predictions obtained from the BPM. A more realistic approach to calculate fusion cross sections takes into account the internal structure of the colliding nuclei, using the CC formalism. In this work, we adopt the zero

Table 3. Total fusion cross section and astrophysical *S*-factor obtained in the present work.

Energy (MeV)	σ_{fus} (mb)	$S(E)$ (MeV b)
8.27	1.64 ± 0.38	$(1.47 \pm 0.33) \times 10^{25}$
9.27	21.1 ± 1.4	$(6.7 \pm 0.5) \times 10^{24}$
10.77	152 ± 7	$(8.0 \pm 0.4) \times 10^{23}$
12.27	407 ± 25	$(7.8 \pm 0.5) \times 10^{22}$

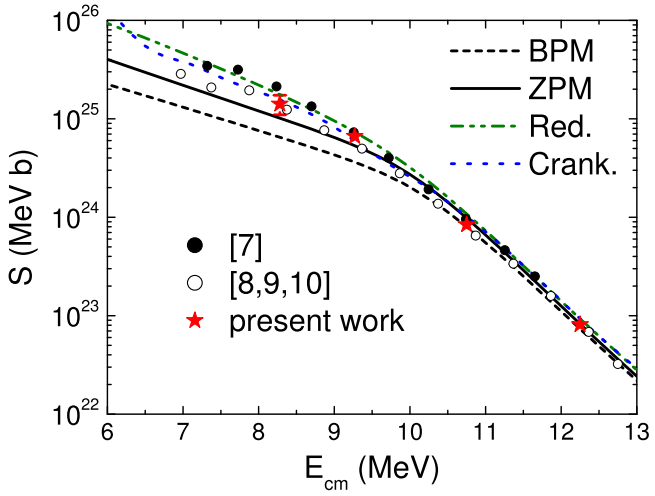

Figure 5. Same as bottom part of figure 4. The red stars refer to the experimental results obtained in the present work. The dashed and solid lines are the results obtained with the BPM and ZPM model, respectively.

point motion (ZPM) model of [26–29], that couples the complete sets of inelastic states related to the quadrupole 2^+ and octopole 3^- vibrational bands. The effect of the couplings is to replace the Coulomb barrier height, which is coupled to an harmonic oscillator, by a set of barriers, where the total transmission coefficient is given by a weighted average of the transmission for each effective barrier. The Coulomb barrier parameters have been obtained using the São Paulo potential [18], which assumes a two-parameter Fermi distribution to describe the density of a given nucleus. In this context, there are no adjustable parameters in our model, so the calculations represent predictions rather than data fits. The agreement between the ZPM calculation and the experimental data obtained in this work is satisfactory over the entire energy region (see figure 5). The ZPM model also provides a good description of the averaged experimental astrophysical *S*-factor for [8–10], even at the lowest measured energy. As expected, the results obtained with the BPM underestimate the cross sections at energies below the Coulomb barrier.

An alternative theoretical model was previously presented in [12], in which molecular effects on the $^{16}O+^{16}O$ reaction were investigated within the two-center shell model (TCSM) based on Woods–Saxon potentials. The results of this work are showed in figure 5, where the dashed green and dotted blue curves refer to the results obtained by considering a constant reduced mass and the radial cranking mass, respectively. At energies around the barrier height ($V_B \simeq 10.2$ MeV), the blue curve presents better agreement with the different data sets in

comparison with the green curve. Subsequently, an overall better accordance between the results obtained by considering the cranking mass (blue curve) and the average value of [8–10] can be observed at sub-barrier energies.

5. Summary and conclusion

The fusion cross section data for $^{16}O+^{16}O$ were obtained using the γ-ray spectroscopy technique. The measurements were performed in the center-of-mass energy range from 8.28 to 12.25 MeV. The partial cross sections for each possible residual nucleus formed in the reaction were experimentally determined, apart from the ^{28}Si channel for which the results were taken from the literature.

The experimental fusion cross sections, represented in terms of the astrophysical *S*-factor, are in good agreement with the theoretical results obtained with the ZPM, which predicts an extrapolated *S*-factor value of 2.8×10^{25} MeV barn at the 6.6 MeV Gamow peak energy. However, a careful inspection of figure 5 shows that the lowest energy cross section data are about 30% larger than that predicted by the ZPM, leading to a *S*-factor value about 3.6×10^{25} MeV barn. The TCSM calculation performed by considering the radial cranking mass gives a *S*-factor value of 5.0×10^{25} MeV barn at $E_{c.m.}$= 6.6 MeV (see blue curve at figure 5). As expected, the calculations (BPM) without taking into account the couplings to the inelastic states of ^{16}O significantly underestimate the data at energies below the Coulomb barrier.

Acknowledgments

This work was partially supported by the Fundação de Amparo à Pesquisa do Estado de São Paulo (FAPESP) and the Conselho Nacional de Desenvolvimento Científico e Tecnológico (CNPq).

References

[1] Barnes C A, Trentalange S and Wu S-C 1985 *Treatise on Heavy Ion Science* vol 6 (New York: Plenum)
[2] Weaver T A and Woosley S E 1993 *Phys. Rep.* **227** 65
[3] Woosley S E, Heger A, Rauscher T and Hoffman R D 2003 *Nucl. Phys.* A **718** 3
[4] Rolfs C E and Rodney W S 1988 *Cauldrons in the Cosmos* (Chicago: University of Chicago Press)
[5] Kovar D G *et al* 1979 *Phys. Rev.* C **20** 1305
[6] Hulke G, Rolfs C and Trautvetter H P 1980 *Z. Phys.* A **297** 161
[7] Spinka H and Winkler H 1974 *Nucl. Phys.* A **233** 456
[8] Kuronen A, Keinonen J and Tikkanen P 1987 *Phys. Rev.* C **35** 591
[9] Thomas J, Chen Y T, Hinds S, Meredith D and Olson M 1986 *Phys. Rev.* C **33** 1679
[10] Wu S-C and Barnes C A 1984 *Nucl. Phys.* A **422** 373
[11] Gasques L R, Brown E F, Chieffi A, Jiang C L, Limongi M, Rolfs C, Wiescher M and Yakovlev D G 2007 *Phys. Rev.* C **76** 035802
[12] Diaz-Torres A, Gasques L R and Wiescher M 2007 *Phys. Lett.* B **652** 255
[13] Balantekin B, Koonin S and Negele J 1983 *Phys. Rev.* C **28** 1565
[14] Gasques L R, Chamon L C, Pereira D, Alvarez M A G, Rossi E S Jr, Silva C P and Carlson B V 2004 *Phys. Rev.* C **69** 034603
[15] Vandenbosch R 1992 *Annu. Rev. Nucl. Part. Sci.* **42** 447
[16] Stefanini A M *et al* 1994 *Proc. Workshop on Heavy Ion Fusion, Exploring the Variety of Nuclear Properties* (Singapore: World Scientific)

[17] Gil S and DiGregorio D E 1997 *Phys. Rev.* C **57** R2826
[18] Chamon L C, Carlson B V, Gasques L R, Pereira D, De Conti C, Alvarez M A G, Hussein M S, Candido Ribeiro M A, Rossi E S Jr and Silva C P 2002 *Phys. Rev.* C **66** 014610
[19] Alcántara-Núñez J A *et al* 2003 *Nucl. Instrum. Methods* A **497** 429
[20] Ribas R *et al* 1996 *Annual Report of the Nuclear Physics Department* (Institute of Physics, University of São Paulo) p 63
[21] Gomes P R S, Penna T J P, Liguori Neto R, Acquadro J C, Tenreiro C, Freitas P A B, Crema E, Carlin Filho N and Coimbra M M 1989 *Nucl. Instrum. Methods* A **280** 395
[22] Hauser W and Feshbach H 1952 *Phys. Rev.* **87** 366
[23] Kis Z, Fazekas B, Östör J, Révay Z, Belgya T, Molnár G L and Koltay L 1998 *Nucl. Instrum. Methods* A **418** 374
[24] Thompson I J 1988 *Comput. Phys. Rep.* **7** 167
[25] Christensen P R, Switkowski Z E and Dayras R A 1977 *Nucl. Phys.* A **280** 189
[26] Dasso C H, Landowne S and Winther A 1983 *Nucl. Phys.* A **407** 221
[27] Nobre G P A, Chamon L C, Gasques L R, Carlson B V and Thompson I J 2007 *Phys. Rev.* C **75** 044606
[28] Nobre G P A, Silva C P, Chamon L C and Carlson B V 2007 *Phys. Rev.* C **76** 024605
[29] Nobre G P A and Chamon L C 2007 *Phys. Rev.* C **76** 044608